

## Corrosion Inhibition of Mild Steel by S-benzyl-O,O'-dialkyldithiophosphates in HCl Solution

Kun Wang<sup>1</sup>, Chuan Lai<sup>1,2\*</sup>, Banglong Tan<sup>3</sup>, Bin Xie<sup>2\*\*</sup>, Shasha Zhu<sup>2</sup>, Hui Zhu<sup>1</sup>, Ke Liu<sup>1</sup>, Jian Wei<sup>2</sup>

<sup>1</sup>School of Chemistry and Chemical Engineering, Eastern Sichuan Sub-center of National Engineering Research Center for Municipal Wastewater Treatment and Reuse, Sichuan University of Arts and Science, Dazhou 635000, PR China

<sup>2</sup> College of Chemistry and Environmental Engineering, Institute of Functional Materials, Material Corrosion and Protection Key Laboratory of Sichuan Province, Sichuan University of Science and Engineering, Zigong 643000, PR China

<sup>3</sup>DaZhou Quality Technical Supervision and Inspection Testing Center, Dazhou 635000, PR China

\*E-mail: [laichuanemail@163.com](mailto:laichuanemail@163.com)

\*\*E-mail: [xiebinsuse@163.com](mailto:xiebinsuse@163.com)

Received: 16 October 2017 / Accepted: 9 December 2017 / Published: 5 February 2018

---

In present work, the target compounds of S-benzyl-O,O'-dialkyldithiophosphates including S-benzyl-O,O'-diphenyldithiophosphate (Inhi-1), S-benzyl-O,O'-dibenzylthiophosphate (Inhi-2), S-benzyl-O,O'-di(2-phenylethyl)dithiophosphate(Inhi-3) and S-benzyl-O,O'-di(4-methylphenyl)dithiophosphate (Inhi-4) were prepared, which acting as corrosion inhibitor for mild steel (MS) in HCl solution were investigated by weight loss measurement, potentiodynamic polarization measurement and electrochemical impedance spectroscopy. The potentiodynamic polarization measurement indicates that the four synthesized compounds are all the mixed-type inhibitor for MS corrosion in HCl solution. Furthermore, all measurements in this study show that the inhibition efficiency increases with inhibitor concentration increasing. Weight loss measurement reveals that inhibition efficiency decreases with HCl concentration and temperature increasing. In addition, the adsorption of Inhi-1, Inhi-2, Inhi-3 and Inhi-4 on MS surface obeys Langmuir isotherm, which are mixed adsorption involving both physisorption and chemisorption.

---

**Keywords:** Acid; Corrosion; Inhibition; Synthesis; Mild steel; Polarization; Adsorption.

### 1. INTRODUCTION

Corrosion is an unavoidable but a controllable process [1]. Corrosion inhibitors are substances which added in corrosive medium with a small concentration to decrease or prevent the corrosion of the metal with aggressive medium [2]. At the present time, a number of organic compounds were

reported as effective corrosion inhibitors for different metals in acid solution as aggressive medium. For example, Lamaka [3] concluded and reported 151 individual compounds including 125 individual organic compounds as the corrosion inhibitor for magnesium and its alloys. Xhanari [4] summarized the research work published in the last two decades on the use of organic compounds (amines, N-heterocyclic compounds,azole, imidazole, thiazole derivatives, different kinds of polymers, organic dyes and Schiff bases) as corrosion inhibitors for aluminium and its alloys in acidic solutions. Finšgar [5] summarized the corrosion inhibition of copper by 1,2,3-benzotriazole and their derivatives. With the further Finšgar [6] also summarized that the corrosion inhibition of steel materials in acidic media by numerous organic inhibitors. As a matter of fact, most of the effective organic corrosion inhibitors are organic compounds, which all contain electronegative atoms (such as, N, P, S and O atoms), the unsaturated bonds (such as, double bonds or triple bonds) and the plane conjugated systems in their molecular structures [7-11]. The corrosion inhibition of these organic compounds is mainly because of physical or chemical adsorption resulting from the interaction of polar centers of the inhibitor with active sites on metal surface [12-15]. As a fact, the O,O'-diaryldithiophosphates their derivatives can act as the potential inhibitors resulting from the N, P, S and O atoms consist in their molecular structures. According to our previous works, the O,O'-dialkyldithiophosphates diethyl ammonium ((RO)<sub>2</sub>PS<sub>2</sub>NH<sub>2</sub>Et<sub>2</sub>) and a part of O,O'-dialkyldithiophosphates covalence compounds also reported as the excellent corrosion inhibitors [16-19].

In order to develop the new effective corrosion inhibitor and extend the investigation by O,O'-dialkyldithiophosphates as corrosion inhibitor, the present work is to investigate the corrosion inhibition of mild steel in hydrochloric acid solution by the covalence compounds of S-benzyl-O,O'-dialkyldithiophosphates including S-benzyl-O,O'-diphenyldithiophosphate (Inhi-1), S-benzyl-O,O'-dibenzyl dithiophosphate (Inhi-2), S-benzyl-O,O'-di(2-phenylethyl)dithiophosphate (Inhi-3) and S-benzyl-O,O'-di(4-methylphenyl)dithiophosphate (Inhi-4).

## 2. MATERIALS AND METHODS

### 2.1 Materials

In this work, all the used reagents and solvents containing P<sub>2</sub>S<sub>5</sub> (phosphorus pentasulphide), 4-MePhOH (4-methylphenol), PhOH (phenol), PhCH<sub>2</sub>OH (benzyl alcohol), PhCH<sub>2</sub>CH<sub>2</sub>OH (phenylethyl alcohol), NHEt<sub>2</sub> (diethylamine), CH<sub>2</sub>Cl<sub>2</sub> (dichloromethane), PhCH<sub>2</sub>Br (benzyl bromide), PhCH<sub>3</sub> (toluene), CH<sub>3</sub>COCH<sub>3</sub> (acetone) and HCl (hydrochloric acid, 37%), were purchased from Sinopharm Chemical Reagent Co., Ltd (China), which were commercially available and analytically pure.

After the target inhibitors of Inhi-1, Inhi-2, Inhi-3 and Inhi-4 synthesized, which would be confirmed by Carlo Erba 1106 instrument (Italy) elemental analysis and Nicolet-6700 FT-IR spectrometer (USA). Meanwhile, the electrochemical methods including potentiodynamic polarization measurement and electrochemical impedance spectroscopy were employed by CHI 660D electrochemical workstation (China). All the rectangle test specimens (5 mm×20 mm×50 mm) and working electrode (0.785 cm<sup>2</sup>) were prepared by mild steel (MS). Electrochemical measurements were

conducted by conventional three-electrode system consisting of the MS working electrode, a counter Pt electrode and a saturated calomel reference electrode (SCE).

In addition, during the whole testing process, temperature was controlled by HH-1 water thermostat (China). The various concentrations of HCl solutions were prepared by HCl (37%) and deionized water.

## 2.2 Synthesis of inhibitors

In order to synthesize the inhibitors of S-benzyl-O,O'-dialkyldithiophosphates including S-benzyl-O,O'-diphenyldithiophosphate (Inhi-1), S-benzyl-O,O'-dibenzoyldithiophosphate (Inhi-2), S-benzyl-O,O'-di(2-phenylethyl)dithiophosphate (Inhi-3) and S-benzyl-O,O'-di(4-methylphenyl)dithiophosphate (Inhi-4), the ammonium salts of  $(RO)_2PS_2NH_2Et_2$  (O,O'-dialkyldithiophosphates diethyl ammonium) as the starting compounds were prepared by reaction of ROH (R=Ph, PhCH<sub>2</sub>, PhCH<sub>2</sub>CH<sub>2</sub> and 4-MePh), P<sub>2</sub>S<sub>5</sub> with NH<sub>2</sub>Et<sub>2</sub> in toluene [16,17]. Then, the target corrosion inhibitors of Inhi-1, Inhi-2, Inhi-3 and Inhi-4 were synthesized by  $(RO)_2PS_2NH_2Et_2$  and benzyl bromide (PhCH<sub>2</sub>Br) in dichloromethane (CH<sub>2</sub>Cl<sub>2</sub>) based on the detailed process described in our previous works [18,19]. The synthetic route and chemical structures of the target corrosion inhibitors are shown in figure 1.

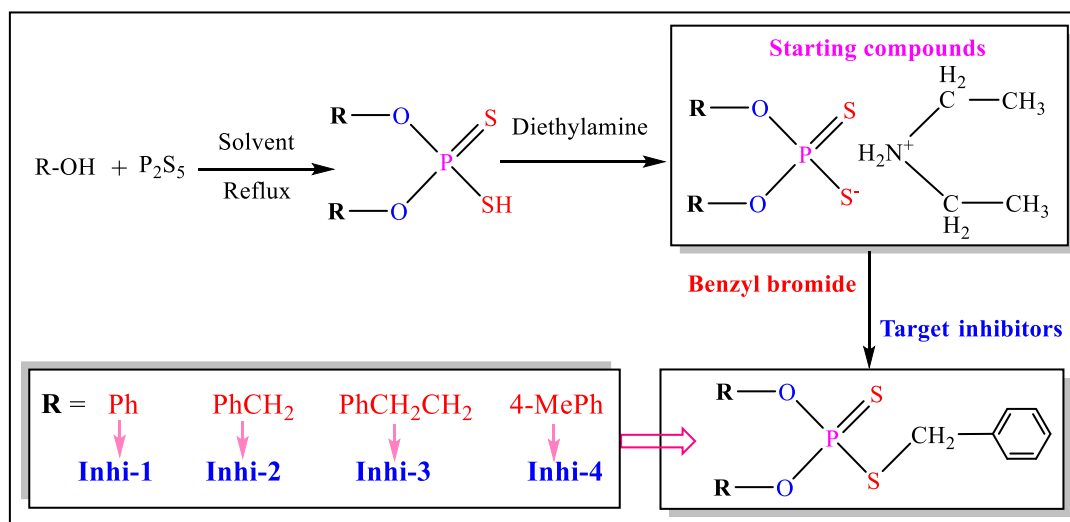


**Figure 1.** The synthetic route and chemical structures of the target corrosion inhibitors

## 2.3 Weight loss measurement

Weight loss measurement as the classical method for corrosion inhibition studying, this method was described in literatures [20-21]. According to this method, in each measurement, at least three closer results were considered, and their average value has been presented. The corrosion rate ( $v$ , g m<sup>-2</sup> h<sup>-1</sup>) and inhibition efficiency ( $IE_{Wt.}(\%)$ ) were calculated from equation (1) and (2). In this work,  $m_1$  and  $m_2$  are the mass of the MS specimen before and after corrosion,  $S$  is the total surface area of the MS

specimen,  $t$  is the immersion time,  $v_0$  and  $v$  are corrosion rate of the MS specimen corrosion in HCl solution in the absence and presence of different concentration of Inhi-1, Inhi-2, Inhi-3 and Inhi-4.

$$v = (m_1 - m_2) / St \quad (1)$$

$$IE_{Wt}(\%) = 100\% \times (v_0 - v) / v_0 \quad (2)$$

### 2.3 Electrochemical measurements

Electrochemical measurements including potentiodynamic polarization measurement (Tafel) and electrochemical impedance spectroscopy (EIS) were conducted by conventional three-electrode system, and all potential in this study were referred to SCE.

Potentiodynamic polarization measurement (Tafel): The potential sweep rate for potentiodynamic polarization measurement to obtain the Tafel curves was  $0.5 \text{ mV s}^{-1}$ . The corrosion current density ( $i_{cor}$ ) was determined from the intercept of extrapolated cathodic and anodic Tafel lines at the corrosion potential ( $E_{cor}$ ). The corresponding inhibition efficiency ( $IE_{Tafel}(\%)$ ) was calculated as equation (3) [17, 22-23]. In this equation,  $i_{cor}$  and  $i_{cor(inh)}$  are the corrosion current density values of MS corrosion in HCl solution in the absence and presence of different concentration of Inhi-1, Inhi-2, Inhi-3 and Inhi-4.

$$IE_{Tafel}(\%) = 100\% \times (i_{cor} - i_{cor(inh)}) / i_{cor} \quad (3)$$

Electrochemical impedance spectroscopy (EIS): EIS was performed in frequency range of 100 kHz to 10 mHz using a sinusoidal AC perturbation with amplitude of 10 mV. Charge transfer resistance ( $R_{ct}$ ) was obtained from the diameter of the semicircle of the Nyquist plot. The corresponding inhibition efficiency ( $IE_{EIS}(\%)$ ) derived from this method was calculated by equation (4) [19, 24].  $R_{ct0}$  and  $R_{ct}$  are the values of charge transfer resistance observed by MS corrosion in HCl solution in the absence and presence of different concentration of Inhi-1, Inhi-2, Inhi-3 and Inhi-4.

$$IE_{EIS}(\%) = 100\% \times (R_{ct} - R_{ct0}) / R_{ct} \quad (4)$$

## 3. RESULTS AND DISCUSSION

### 3.1 Characterization

**Table 1.** The elemental analysis data of the target inhibitors Inhi-1, Inhi-2, Inhi-3 and Inhi-4

Inhibitor	Molecular Formula	Anal. Calcd			Anal. Found		
		C (%)	H (%)	S (%)	C (%)	H (%)	S (%)
Inhi-1	C <sub>19</sub> H <sub>17</sub> O <sub>2</sub> PS <sub>2</sub> (372)	61.27	4.60	17.22	61.25	4.62	17.21
Inhi-2	C <sub>21</sub> H <sub>21</sub> O <sub>2</sub> PS <sub>2</sub> (401)	62.98	5.29	16.01	62.99	5.27	16.02
Inhi-3	C <sub>23</sub> H <sub>25</sub> O <sub>2</sub> PS <sub>2</sub> (429)	64.46	5.88	14.96	64.43	5.89	14.95
Inhi-4	C <sub>21</sub> H <sub>21</sub> O <sub>2</sub> PS <sub>2</sub> (401)	64.46	5.88	14.96	64.48	5.86	14.98

In order to analyze the molecular structure of synthesized corrosion inhibitors, the elemental analysis and FT-IR were employed to confirm the chemical structural of Inhi-1, Inhi-2, Inhi-3 and Inhi-4. The characterization results of elemental analysis were presented in table 1, and FT-IR results shown in table 2 and figure 2.

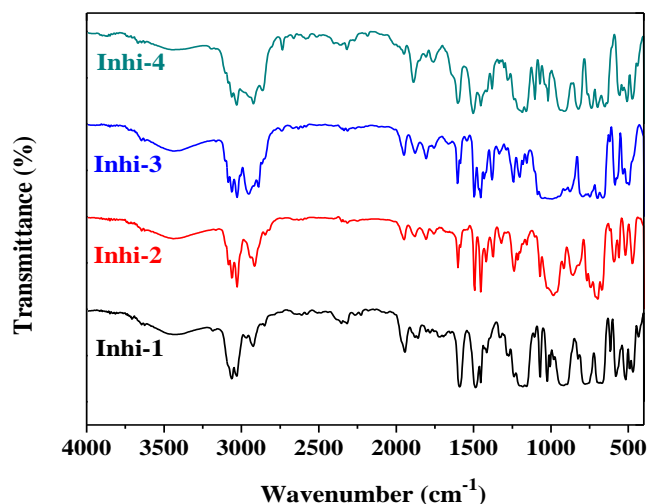


**Figure 2.** Infrared spectra of the target inhibitors Inhi-1, Inhi-2, Inhi-3 and Inhi-4

**Table 2.** The infrared spectra data of the target inhibitors Inhi-1, Inhi-2, Inhi-3 and Inhi-4

Inhibitor	Wavenumber ( $\tilde{\nu}$ , $\text{cm}^{-1}$ )					
	(=C-H)	(C=C)	((P)-O-C)	(P-O-(C))	(S-C)	(PS <sub>2</sub> )
Inhi-1	3062.7 (s), 3030.1 (s).	1453.8 (s), 1487.0 (s), 1590.0 (s).	1181.6 (s), 1238.4 (m).	914.5 (m), 1024.4 (s), 1070.2 (s).	875.6 (m)	671.4 (s), 779.1 (s), 517.7 (s), 580.6 (s).
Inhi-2	3028.2 (s), 3061.0 (m).	1453.0 (s), 1486.1 (s), 1493.6 (s).	1214.2 (m), 1238.5 (s).	984.9 (s), 1070.6 (s).	856.3 (m)	670.5 (s), 698.2 (s), 743.5 (s), 519.0 (m), 592.4 (m).
Inhi-3	3028.2 (s), 3084.9 (m).	1453.7 (s), 1495.3 (s), 1602.9 (m).	1202.0 (m), 1243.1 (s).	910.3 (s), 994.5 (s), 1086.0 (s).	876.5 (s)	664.9 (s), 699.3 (s), 748.6 (s), 495.4 (s), 586.5 (s).
Inhi-4	3030.8 (s), 3061.8 (s).	1453.2 (s), 1502.9 (s), 1601.4 (s).	1160.3 (s), 1185.8 (s).	914.1 (s), 1018.5 (m).	823.4 (s)	652.6 (s), 698.9 (s), 738.0 (s), 508.1 (s), 535.9 (s), 556.7 (s).

w=weak, s=strong, m=medium.

From the results of elemental analysis listed in table 1, it can be found that the calculated and observed elemental analysis data for the synthesized inhibitors of Inhi-1, Inhi-2, Inhi-3 and Inhi-4 are in good agreement and fit well the structure of target corrosion inhibitor showing in figure 1. Meanwhile, the Fourier transform infrared spectrometer (FT-IR) results were further confirmed that the structures of the target corrosion inhibitors are also in good agreement the structure of Inhi-1, Inhi-2, Inhi-3 and Inhi-4.

### 3.2 Weight loss measurement

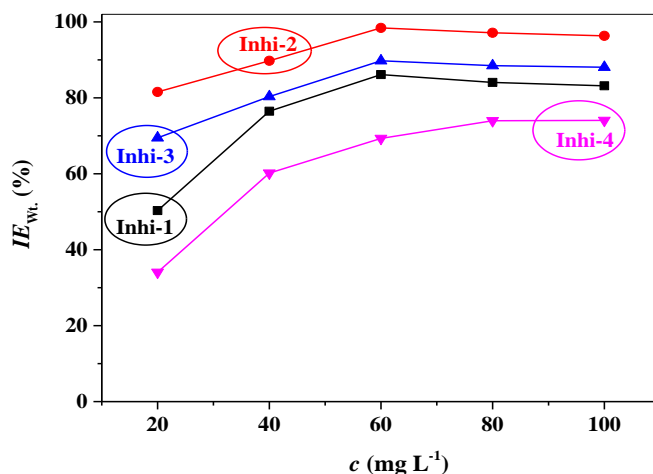


**Figure 3.** The effect of target inhibitors concentration ( $c$ ) on corresponding inhibition efficiency ( $IE_{Wt.}$ (%)) for MS in 1.0 M HCl at 303 K from weight loss measurement

Based on weight loss measurement, the results of the effect of target inhibitors (Inhi-1, Inhi-2, Inhi-3 and Inhi-4) concentration on corresponding inhibition efficiency ( $IE_{Wt.}$ %) for MS in 1.0 M HCl at 303 K were exhibited in figure 3. From this figure, it can be seen clearly that the inhibition efficiency increase with concentration of Inhi-1, Inhi-2, Inhi-3 and Inhi-4 increasing, when the concentration of inhibitor increase to 60 mg L<sup>-1</sup>, the inhibition efficiency change slightly with inhibitor concentration further increase. This is due to the surface coverage of the inhibitors on MS surface increase with the four inhibitors concentration increasing. The result also shows that the inhibition efficiency of the investigated compounds follow the order of Inhi-2 > Inhi-3 > Inhi-1 > Inhi-4. With the concentration of Inhi-1, Inhi-2, Inhi-3 and Inhi-4 increase to 100 mg L<sup>-1</sup>, the inhibition efficiencies are 83.2%, 96.3%, 88.1% and 74.1%, which further demonstrate that the inhibitor of Inhi-2 and Inhi-3 can act as an effective corrosion inhibitor for MS steel in HCl solution. The inhibition behavior of MS by Inhi-2 and Inhi-3 in HCl solution can be attributed to the adsorption of components on MS surface, which retards the dissolution of MS by blocking its active corrosion sites.

### 3.3 Potentiodynamic polarization measurement

At 303 K, all polarization curves (Tafel curves) of MS in 1.0 M HCl with various concentrations of Inhi-1, Inhi-2, Inhi-3 and Inhi-4 obtained from potentiodynamic polarization measurement were presented in figure 4 (a), (b), (c) and (d), respectively. According to this method, the electrochemical parameters of MS corrosion in 1.0 M HCl with different concentrations of Inhi-1, Inhi-2, Inhi-3 and Inhi-4 including corrosion current density  $I_{cor}$  ( $\mu A cm^{-2}$ ), corrosion potential  $E_{cor}$  (vs SCE, mV), cathodic and anodic Tafel slopes  $\beta_c$  and  $\beta_a$  (mV dec<sup>-1</sup>) and the corresponding inhibition efficiency ( $IE_{Tafel}$ (%)) were listed in table 3.

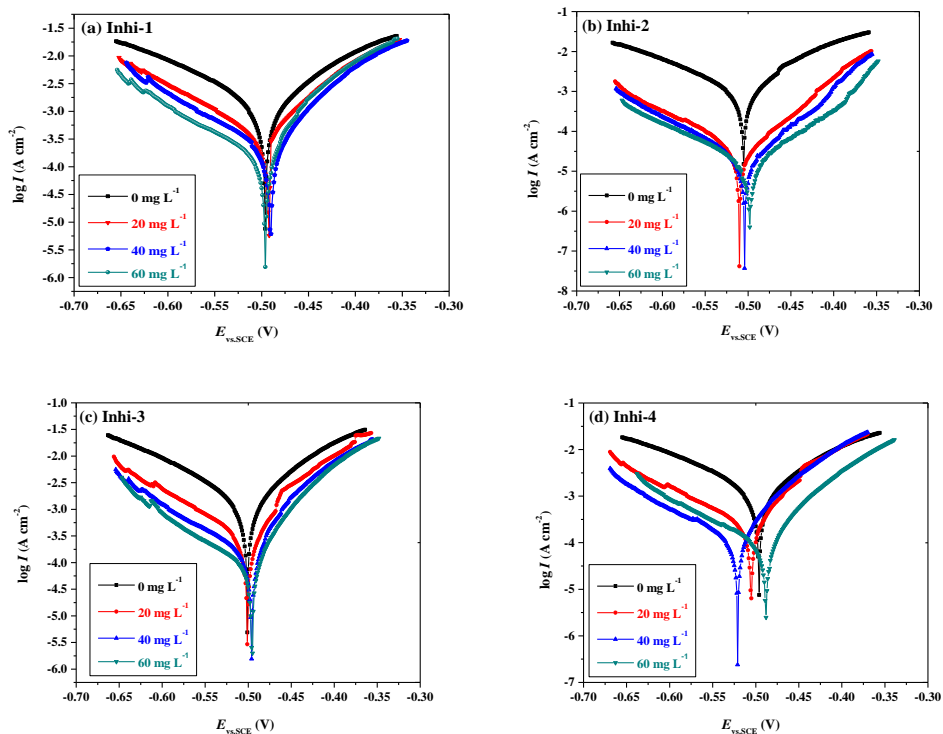


**Figure 4.** The potentiodynamic polarization curves for MS in 1.0 M HCl in the absence and presence of different concentrations of Inhi-1 (a), Inhi-2 (b), Inhi-3 (c) and Inhi-4 (d) at 303K

**Table 3.** The polarization parameters and corresponding inhibition efficiency ( $IE_{Tafel}(\%)$ ) for mild steel in 1.0 M HCl in the absence and presence of different concentrations of Inhi-1, Inhi-2, Inhi-3 and Inhi-4 at 303 K

Inhibitor	$c$ ( $\text{mg L}^{-1}$ )	$E_{cor}$ (mV)	$I_{cor}$ ( $\mu\text{A cm}^{-2}$ )	$\beta_a$ ( $\text{mV dec}^{-1}$ )	$\beta_c$ ( $\text{mV dec}^{-1}$ )	$IE_{Tafel}$ (%)
Blank solution	0	-496	1968.15	131.2	113.3	
Inhi-1	20	-495	1023.18	126.4	93.37	48.0
	40	-491	754.34	101.63	84.39	61.7
	60	-490	393.50	82.44	75.93	80.0
Inhi-2	20	-510	344.19	104.8	63.78	82.2
	40	-504	172.37	102.6	49.80	91.2
	60	-498	22.03	93.63	47.28	98.9
Inhi-3	20	-501	560.76	115.5	93.02	71.5
	40	-496	308.28	96.71	87.18	84.3
	60	-495	194.27	84.32	73.58	90.1
Inhi-4	20	-496	1208.69	125.5	101.5	38.6
	40	-492	627.90	122.1	99.30	68.1
	60	-488	509.87	107.9	97.85	74.1

According to figure 4 (a)-(d) and table 3, it can be found that both the anodic and cathodic curves shift to lower current densities after addition of Inhi-1, Inhi-2, Inhi-3 and Inhi-4 in 1.0 M HCl, which indicate that the four inhibitors all can reduce the MS anodic dissolution and retard the

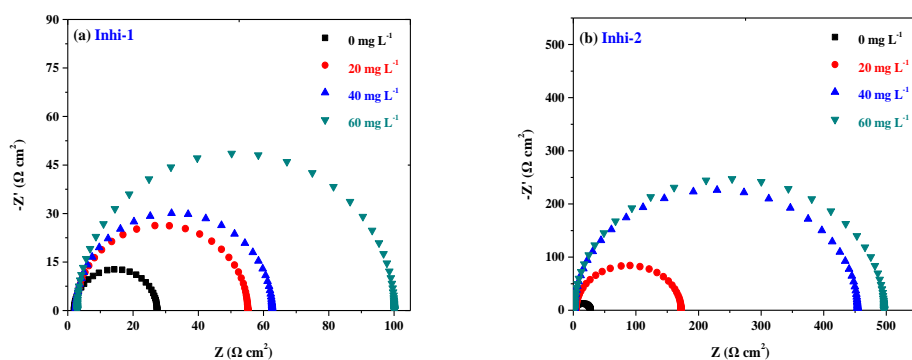
hydrogen ion reduction. The inhibition effect enhances with the increase of Inhi-1, Inhi-2, Inhi-3 and Inhi-4 concentration, resulting from the adsorption of inhibitors on the MS electrode surface. The possible mechanism is the adsorption of the inhibitors on MS surface through the electron pair of heteroatoms (S and O), and the  $\pi$  electron of benzene rings in the molecular structure of Inhi-1, Inhi-2, Inhi-3 and Inhi-4, which can block the MS surface and reduces the corrosive attraction of MS in the aggressive media of HCl solution.

Furthermore, according to table 3, it is obvious that the corrosion current density is much smaller in the presence of Inhi-1, Inhi-2, Inhi-3 and Inhi-4 comparing with that in the absence of Inhi-1, Inhi-2, Inhi-3 and Inhi-4 for MS in 1.0 M HCl, and which decreases with inhibitors concentration increasing. The inhibition efficiency increase with inhibitors concentration increasing is due to the increase of the blocked fraction of the MS electrode surface by adsorption. With Inhi-1, Inhi-2, Inhi-3 and Inhi-4 concentration increase to  $60 \text{ mg L}^{-1}$ , the inhibition efficiencies are 80.0%, 98.9%, 90.1% and 74.1%, this result also reveal that the Inhi-2 and Inhi-3 can act as good corrosion inhibitor for MS in 1.0 M HCl, and the performance of corrosion inhibition for MS in 1.0 M HCl by Inhi-2 higher than others. These results are in good agreement with the results obtained from weight loss measurement.

In addition, based on potentiodynamic polarization measurement, the corrosion inhibitor can be classified as cathodic or anodic type if the displacement in corrosion potential is more than 85 mV with respect to corrosion potential of the HCl blank solution [7, 16, 19]. According to the polarization curves showing in figure 4 (a)-(d) and the polarization parameters listing in table 3, it can be found that the corrosion potentials shift slightly in the negative direction. All corrosion potential of MS in 1.0 M HCl with Inhi-1, Inhi-2, Inhi-3 and Inhi-4 at 303 K shifts less than 85 mV, which indicate that the Inhi-1, Inhi-2, Inhi-3 and Inhi-4 are mixed-type inhibitor.

### 3.4 Electrochemical impedance spectroscopy

According to equivalent circuit mode showing in figure 6, the Nyquist diagrams of MS in 1.0 M HCl with various concentrations of Inhi-1, Inhi-2, Inhi-3 and Inhi-4 at 303 K from EIS were shown in figure 5 (a), (b), (c) and (d).





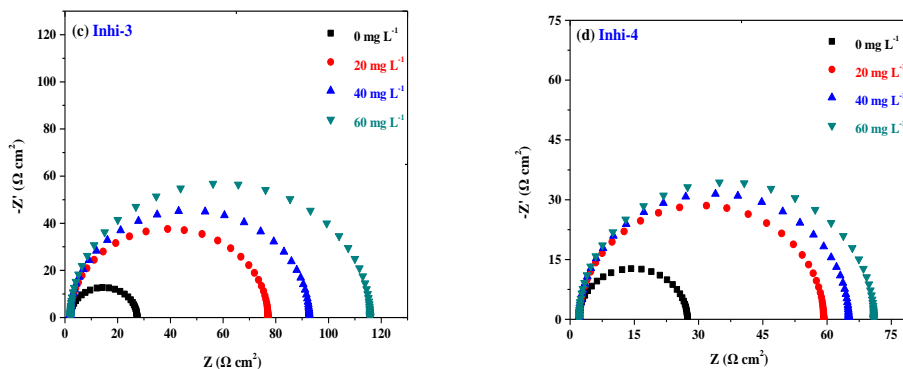


**Figure 5.** The Nyquist plots for MS in 1.0 M HCl in the absence and presence of different concentrations of Inhi-1(a), Inhi-2(b), Inhi-3(c) and Inhi-4(d) at 303 K

Furthermore, the electrochemical parameters of impedance involving the double layer capacitance ( $C_{dl}$ ), charge transfer resistance ( $R_{ct}$ ) and the corresponding inhibition efficiency ( $IE_{EIS}(\%)$ ) obtained from this method were listed in table 4.

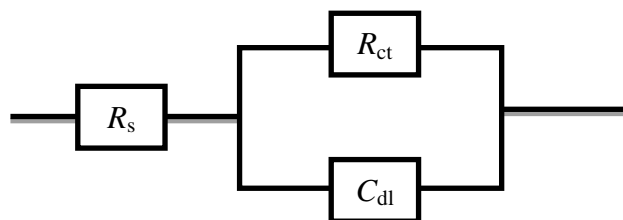


**Figure 6.** Equivalent circuit mode

**Table 4.** The electrochemical parameters of impedance and corresponding inhibition efficiency ( $IE_{EIS}(\%)$ ) for MS in 1.0 M HCl in the absence and presence of different concentrations of Inhi-1, Inhi-2, Inhi-3 and Inhi-4 at 303 K

Inhibitor	$c$ ( $\text{mg L}^{-1}$ )	$R_{ct}$ ( $\Omega \text{ cm}^{-2}$ )	$C_{dl}$ ( $\mu\text{F cm}^{-2}$ )	$IE_{EIS}$ (%)
Blank solution	0	25.44	78.36	
Inhi-1	20	52.64	33.55	51.7
	40	60.17	27.76	57.7
	60	101.31	22.71	74.9
Inhi-2	20	168.1	11.16	84.9
	40	336.8	5.33	92.5
	60	452.1	2.24	94.4
Inhi-3	20	75.07	22.03	66.1
	40	90.70	15.79	72.0
	60	178.4	15.04	85.7
Inhi-4	20	57.01	27.43	36.5
	40	65.90	25.63	61.4
	60	78.79	24.86	67.7

From figure 5 (a)-(d), it can be found that all the Nyquist plots show a single capacitive loop, in 1.0 M HCl as blank solution and aggressive media with inhibitors (HCl+Inhi-1, Inhi-2, Inhi-3 or Inhi-4), which is attributed to the charge transfer of corrosion process. The impedance spectra show that the single semicircle and the diameter of semicircle increase with the concentration of all inhibitors. According to table 4, it reveals that the double layer capacitance decrease and charge transfer resistance increase with the concentration of the four inhibitors increasing. The decrease of double layer capacitance may be due to the decrease of the local dielectric constant or the increase of the thickness of the electrical double layer, indicating that the inhibitors adsorbed on the MS surface. The increase of charge transfer resistance can be attributed to the formation of protective film on the MS/solution interface. The inhibition efficiencies recorded by EIS are 74.9%, 94.4%, 85.7% and 67.7% for MS in 1.0 M HCl with 60 mg L<sup>-1</sup> Inhi-1, Inhi-2, Inhi-3 and Inhi-4, respectively. This results obtained from EIS also are in good agreement with the results obtained from weight loss and Tafel measurement.

### 3.5 Adsorption isotherm

The adsorption isotherm can be used to analyze the interaction of the Inhi-1, Inhi-2, Inhi-3 and Inhi-4 on MS surface. Usually, both the physisorption and chemisorption as two main types of interaction are used to describe the adsorption of inhibitors on different metals surface.

In order to confirm the reasonable adsorption isotherm for Inhi-1, Inhi-2, Inhi-3 and Inhi-4 on MS surface in HCl solution, various isotherms including Frumkin, Flory–Huggins, Temkin and Langmuir adsorption isotherms are employed according to the data of weight loss measurement from figure 3. Fitting results reveal that the adsorption of Inhi-1, Inhi-2, Inhi-3 and Inhi-4 on MS surface obey Langmuir adsorption isotherm showing in equation (5) [19]. In this equation, *c* is the concentration of Inhi-1, Inhi-2, Inhi-3 and Inhi-4, *K<sub>A</sub>* is the adsorption equilibrium constant and *θ* is the surface coverage. The surface coverage (*θ*) for different concentrations of Inhi-1, Inhi-2, Inhi-3 and Inhi-4 in 1.0 M HCl is obtained based on equation (6). In equation (6), *v<sub>0</sub>* and *v* are corrosion rate of the MS in HCl solution without and with different concentrations of Inhi-1, Inhi-2, Inhi-3 and Inhi-4.

$$c/\theta = 1/K_A + c \tag{5}$$

$$\theta = (v_0 - v)/v_0 \tag{6}$$

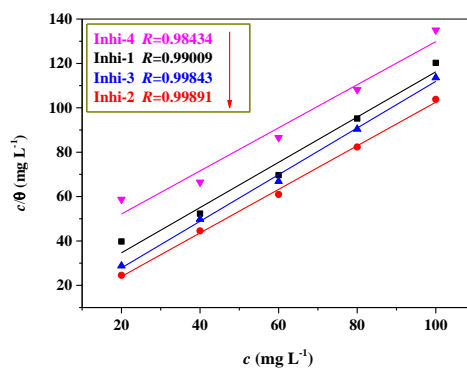


**Figure 7.** Langmuir adsorption isotherm of Inhi-1, Inhi-2, Inhi-3 and Inhi-4 on MS in 1.0 M HCl at 303 K from weight loss measurement

The plots of  $c/\theta$  versus  $c$  yield the straight lines shown in figure 7. While the strong correlation ( $R>0.98434$ , see figure 7) suggest that the adsorption of Inhi-1, Inhi-2, Inhi-3 and Inhi-4 on MS surface in 1.0 M HCl obey Langmuir adsorption isotherm. And the standard free energy of adsorption ( $\Delta G_A$ ) can be determined from the intercepts of the straight lines according to equation (7). In this equation,  $R=8.314 \text{ J K}^{-1} \text{ mol}^{-1}$  is the gas constant,  $T$  is absolute temperature (K) and 55.5 is the molar concentration of water in the solution expressed in molarity units ( $\text{mol L}^{-1}$ ).

$$K_A = \exp(-\Delta G_A/RT) \times 1/55.5 \tag{7}$$

Based on equation 7, the obtained values of  $K_A$  and  $\Delta G_A$  for Inhi-1, Inhi-2, Inhi-3 and Inhi-4 were listed in table 5, as can be seen that the calculated values of  $\Delta G_A$  for Inhi-1, Inhi-2, Inhi-3 and Inhi-4 all higher than  $-40.00 \text{ kJ mol}^{-1}$ , which are  $-35.74$ ,  $-38.93$ ,  $-37.95$  and  $-33.83 \text{ kJ mol}^{-1}$ , and it also indicates that the adsorption processes of Inhi-1, Inhi-2, Inhi-3 and Inhi-4 on MS surface in 1.0 M HCl belongs to mixed adsorption involving both physisorption and chemisorption [19, 25-26].

**Table 5.** Thermodynamic parameters for the adsorption of Inhi-1, Inhi-2, Inhi-3 and Inhi-4 on MS in 1.0 M HCl at 303 K from weight loss measurement

Inhibitor	Equation $y = a + b*x$	Intercept	$K_A$ (* $10^4 \text{ M}^{-1}$ )	$\Delta G_A$ ( $\text{kJ mol}^{-1}$ )
Inhi-1	$y=14.2619+1.01951*x$	14.2619	2.608	-35.74
Inhi-2	$y=4.32921+0.98192*x$	4.32921	9.263	-38.93
Inhi-3	$y=6.83309+1.05085*x$	6.83309	6.278	-37.95
Inhi-4	$y=32.72319+0.971*x$	32.7232	1.225	-33.83

### 3.6 Effect of temperature

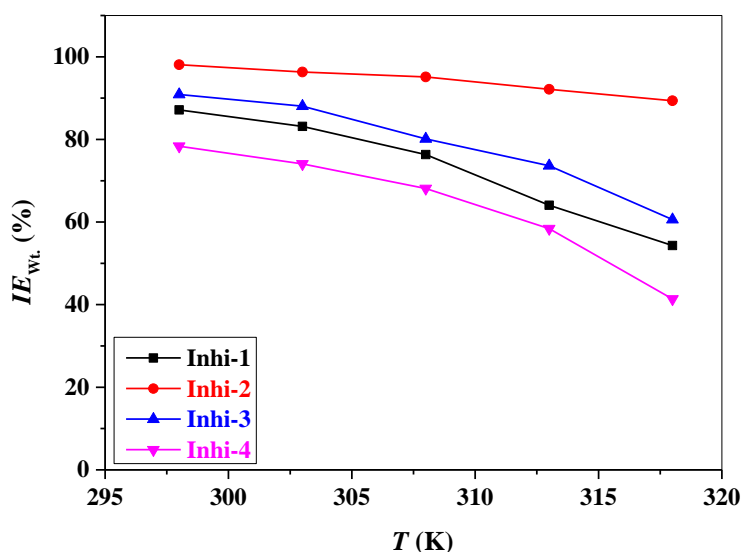


**Figure 8.** The effect of temperature ( $T$ ) on inhibition efficiency ( $IE_{wt.}(\%)$ ) for MS corrosion 1.0 M HCl at 303 K from weight loss measurement

The effect of temperature ( $T$ , K) on corresponding inhibition efficiency ( $IE_{wt.}(\%)$ ) from weight loss measurement were presented in figure 8. From this figure, as can be seen in 1.0 M HCl with 60 mg L<sup>-1</sup> Inhi-1, Inhi-2, Inhi-3 and Inhi-4, the inhibition efficiency decrease with temperature increasing, with temperature increase from 298 K to 318 K that the inhibition efficiency of Inhi-1, Inhi-2, Inhi-3 and Inhi-4 drop from 87.1%, 98.1%, 90.9%, 78.4% (298K) to 54.3%, 89.4%, 60.6%, 41.4%, respectively. The decrease of inhibition efficiency is due to the increasing of inhibitor molecules desorption from MS surface in HCl solution. Compare the mild steel inhibitor of 2-(p-bromobenzylthio)-1*H*-benzimidazole and N,N-diethylammonium O,O'-di(p-methoxyphenyl)dithiophosphate in our previous work [27-28] with the compounds of Inhi-1, Inhi-2, Inhi-3 and Inhi-4 in this work, it is clearly that the effect of temperature on inhibition efficiency have a same influence tendency.

### 3.7 Effect of HCl concentration

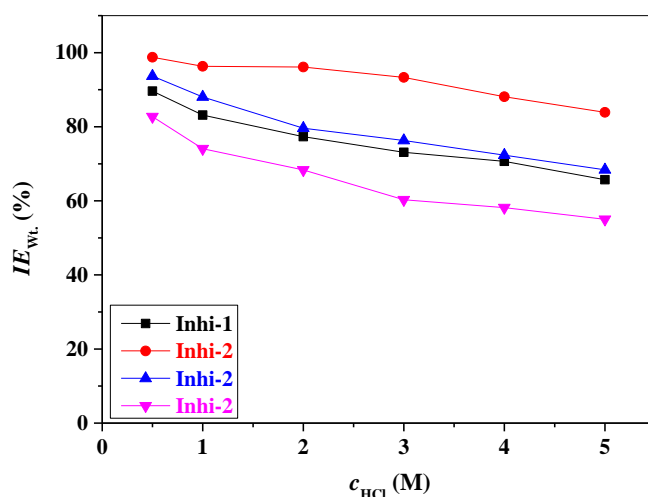


**Figure 9.** The effect of HCl concentration ( $c_{HCl}$ ) on inhibition efficiency ( $IE_{wt.}(\%)$ ) for MS corrosion at 303 K from weight loss measurement

In addition, the effect of HCl concentration ( $c_{HCl}$ , M) on corresponding inhibition efficiency ( $IE_{wt.}(\%)$ ) at 303 K from weight loss measurement were shown in figure 9. From figure 9, it is obvious that the inhibition efficiency decrease with HCl concentration increasing, and the inhibition efficiency of Inhi-1, Inhi-2, Inhi-3 and Inhi-4 (60 mg L<sup>-1</sup>) for MS corrosion in 0.5 M and 5.0 M HCl at 303 K are 89.6%, 98.8%, 93.7%, 82.7% and 65.7%, 83.9%, 68.4%, 55.0%, respectively. The decrease of the inhibition efficiency by increase of HCl concentration is contributed to the increase of hydrogen ion concentration in HCl solution. The similar results were reported by Lai [29] based on N,N-diethylammonium O,O'-di(4-bromophenyl)dithiophosphate as mild steel inhibitor in H<sub>2</sub>SO<sub>4</sub> solution.

## 4. CONCLUSIONS

In conclusion, the corrosion inhibitors of S-benzyl-O,O'-diphenyldithiophosphate (Inhi-1), S-benzyl-O,O'-dibenzylidithiophosphate (Inhi-2), S-benzyl-O,O'-di(2-phenylethyl)dithiophosphate (Inhi-

3) and S-benzyl-O,O'-di(4-methylphenyl) dithiophosphate (Inhi-4) were synthesized and confirmed by elemental analysis and FT-IR in this work. The four synthesized target corrosion inhibitors are mixed-type inhibitor. The inhibition efficiency increases with inhibitor concentration increasing, and decreases with HCl concentration and temperature increasing for mild steel in HCl solution. In addition, the adsorption of Inhi-1, Inhi-2, Inhi-3 and Inhi-4 on mild steel surface obeys Langmuir isotherm, which are mixed adsorption involving both physisorption and chemisorption.

#### ACKNOWLEDGMENTS

This project is supported financially by the program of Science and Technology Department of Sichuan Province (Nos. 2017JY0180, 2016JY0048), the project of Dazhou City (No. KJJ2016002), the program of Education Department of Sichuan Province (No. 17ZB0380), the opening project of Material Corrosion and Protection Key Laboratory of Sichuan Province (No. 2017CL02), the project of Key Laboratories of Fine Chemicals and Surfactants in Sichuan Provincial Universities (No. 2016JXZ03), and the Projects of Zigong Science & Technology and Intellectual Property Bureau (Nos. 2015HX18, 2015CXM01).

#### References

1. D. Kesavan, M. Gopiraman and N. Sulochana, *Che. Sci. Rev. Lett.*, 1 (2012) 1.
2. B. Sanyal, *Pro. Org. Coat.*, 9(1981) 165.
3. S.V. Lamaka, B. Vaghefinazari, D. Mei, R.P. Petrauskas, D. Höche and M.L. Zheludkevich, *Corros. Sci.*, 128 (2017) 224.
4. K. Khanari and M. Finšgar, *Rsc Adv.*, 6 (2016) 62833.
5. M. Finšgar and I. Milošev, *Corros. Sci.*, 52 (2010) 2737.
6. M. Finšgar and J. Jackson, *Corros. Sci.*, 86 (2014) 17.
7. Y. Qiang, S. Zhang, S. Yan, X. Zou and S. Chen, *Corros. Sci.*, 126 (2017) 295.
8. R.K. Gupta, M. Malviya, C. Verma and M.A. Quraishi, *Mater. Chem. Phys.*, 198 (2017) 360.
9. Z. Xiao, H. Wu, G. Liang and D. Zhan, *Int. J. Electrochem. Sci.*, 12 (2017) 10969.
10. Z. Wang, W. Bai, C. Xu, Y. Shi, Y. Wu, J. Guo and L. Feng, *Int. J. Electrochem. Sci.*, 12 (2017) 10291.
11. M.E. Elshakre, H.H. Alalawy, M.I. Awad and B.E. El-Anadouli, *Corros. Sci.*, 124 (2017) 121.
12. M. Mobin, R. Aslam and J. Aslam, *Mater. Chem. Phys.*, 191 (2017) 151.
13. Y. Wu, Y.L. Shi, C.W. Su, L.L. Feng, J.M. Guo and W. Bai, *Int. J. Electrochem. Sci.*, 12 (2017) 10042.
14. B.A. Sami, *Int. J. Electrochem. Sci.*, 12 (2017) 10369.
15. Q. Ma, S. Qi, X. He, Y. Tang and G. Lu, *Corros. Sci.*, 129 (2017) 91.
16. X.L. Su, C. Lai, L.C. Peng, H. Zhu, L.S. Zhou, L. Zhang, X.Q. Liu and W. Zhang, *Int. J. Electrochem. Sci.*, 11 (2016) 4828.
17. C. Lai, X.L. Su, T. Jiang, L.S. Zhou, B. Xie, Y.L. Li and L.K. Zou, *Int. J. Electrochem. Sci.*, 11 (2016) 9413.
18. C. Lai, J. Wei, X. Guo, B. Xie, L. Zou, X. Ma, S. Zhu, L. Chen and G. Luo, *Int. J. Electrochem. Sci.*, 12 (2017) 10457.
19. C. Lai, B. Xie, L. Zou, Z. Xiang, X. Ma and S. Zhu, *Res. Phys.*, 7 (2017) 3434.
20. Y. Elkhotfi, I. Forsal, E.M. Raki and B. Mernari, *J. Adv. Electrochem.*, 3 (2017) 141.
21. M.M. Solomon, H. Gerengi, T. Kaya, E. Kaya and S.A. Umoren, *Cellulose*, 24 (2017) 931.
22. Y. Wan, Z. Qin, Q. Xu, M. Chen, Y. Min and M. Li, *Int. J. Electrochem. Sci.*, 12 (2017) 10701.
23. M. Saida, H. Djahida, B. Leila and B. Zohra, *Int. J. Electrochem. Sci.*, 12 (2017) 11042.
24. A.S. Fouda, F.M. El-Taweel and M. Elgamil, *Int. J. Electrochem. Sci.*, 12 (2017) 11397.

25. V.R. Saliyan and A.V. Adhikari, *Corros. Sci.*, 50 (2008) 55.
26. A.M. Fekry and R.R. Mohamed, *Electrochim. Acta*, 55 (2010) 1933.
27. C. Lai, B. Xie, C. Liu, W. Gou, L. Zhou, X. Su and L. Zou, *Int. J. Corros.*, 2016 (2016) 1.
28. C. Lai, H. Yang, X. Guo, X. Su, L. Zhou, L. Zhang and B. Xie, *Int. J. Electrochem. Sci.*, 11 (2016) 10462.
29. C. Lai, X. Su, T. Jiang, Lvshan Zhou, B. Xie, Y. Li and Like Zou, *Int. J. Electrochem. Sci.*, 11 (2016) 9413.

© 2018 The Authors. Published by ESG ([www.electrochemsci.org](http://www.electrochemsci.org)). This article is an open access article distributed under the terms and conditions of the Creative Commons Attribution license (<http://creativecommons.org/licenses/by/4.0/>).